의학석사 학위논문

Effects of Thyroid Stimulating Hormone on Tumor Growth by Modulating Tumor Microenvironment in Thyroid Cancer

갑상선자극호르몬이 종양 미세환경 조절을 통해 갑상선암의 성장에 미치는 영향

2016 년 2 월

서울대학교 대학원

의학과 중개의학 전공

송 영 신

갑상선자극호르몬이
종양 미세환경 조절을 통해
갑상선암의 성장에 미치는 영향

지도교수 박 영 주

이 논문을 의학석사 학위논문으로 제출함

2015 년 10 월

서울대학교 대학원

의학과 중개의학 전공

송 영 신

송영신의 의학석사 학위논문을 인준함

2016 년 1 월

위 원 장 박 도 준 (인)

부위원장 박 영 주 (인)

위 원 윤 혜 원 (인)

Effects of Thyroid Stimulating Hormone on Tumor Growth by Modulating Tumor Microenvironment in Thyroid Cancer

by

Young Shin Song

A thesis submitted to the Department of Medicine in partial fulfillment of the requirements for the Degree of Master of Science in Medicine (Translational Medicine) at Seoul National University College of Medicine

January 2016

Approved by Thesis Committee:

Professor Do Joon Park Chairman

Professor Young Joo Park Vice chairman

Professor Hyewon Youn

Abstract

Effects of Thyroid Stimulating Hormone on Tumor Growth by Modulating Tumor Microenvironment in Thyroid Cancer

Young Shin Song
Major in Translational Medicine
Department of Medicine
Seoul National University Graduate School

Introduction: The stimulatory effect of thyroid stimulating hormone (TSH) through TSH receptor signal pathways on the growth of thyrocytes is well-demonstrated. Differentiated thyroid cancer (DTC) expresses TSH receptors and retains responsiveness to TSH. Thus, TSH suppression has been used as an important and effective treatment in patients with DTC. Since tumor microenvironment including angiogenesis has a crucial role in cancer

progression and metastasis, we investigated whether the effects of TSH on tumor growth are also mediated by tumor microenvironment using a mouse model of DTC.

Materials and Methods: BHP10-3SC DTC cells, which express TSH receptors, were subcutaneously implanted on 7-week-old BALB/c nu/nu mice. When the greater diameter of tumor became 5 mm or larger, recombinant human TSH (rhTSH, 1.5 μg/g) or vehicle was started to be injected intraperitoneally. Tumor size was measured every 3 days. After 15 days, tumor histology was examined and vascular endothelial growth factor (VEGF) mRNA expression was analyzed using real time-PCR. For supporting *in vivo* results, *in vitro* experiments to demonstrate TSH effects on angiogenesis were performed in BHP10-3SC and human endothelial cells.

Results: Tumors in rhTSH group grew more rapidly than controls, and there was a significant difference in the tumor volume (on day 15, 1733.4 ± 793.5 mm^3 vs. 1148.8 ± 471.1 mm^3, respectively, $P = 0.010$). The vascular density in tumors was significantly increased in rhTSH group (13.8 ± 0.8% vs. 5.7 ± 0.8% in control, $P = 0.021$). Moreover, more tortuous and dilated vessels were observed in tumors of rhTSH group compared with controls (23.0 ± 1.7 μm vs. 7.4 ± 0.5 μm in vascular diameter, respectively, $P < 0.001$). In addition, the

macrophage infiltration in tumors was significantly increased in rhTSH group (27.6 ± 11.6% vs. 12.1 ± 4.3% in control, P = 0.004). *In vitro* experiments showed that TSH induced a significant up-regulation of VEGF-A mRNA expression in BHP10-3SC cells. Conditioned medium of TSH-treated BHP10-3SC cells (TSH-CM) contained higher concentration of VEGF-A than saline-treated CM (control-CM). Finally, treatment of TSH-CM significantly enhance potentials of cell migration and tube formation in human endothelial cells, HMVEC or HUVEC.

Conclusions: TSH supports the growth of thyroid cancer via enhancing abnormal vasculature and subsequent recruitment of macrophages in tumor microenvironments.

Keywords: thyroid stimulating hormone, thyroid cancer, tumor growth, angiogenesis, microenvironment, macrophage

Student number: 2014-21161

CONTENTS

LIST OF FIGURES

LIST OF ABBREVIATIONS

TSH: thyroid stimulating hormone

DTC: differentiated thyroid cancer

AC: adenylate cyclase

PKA: protein kinase A

PLC: phospholipase C

PKC: protein kinase C

VEGF: vascular endothelial growth factor

TAM: tumor-associated macrophage

RPMI: Roswell Park Memorial Institute

FBS: fetal bovine serum

STR: short tandem repeat

PBS: phosphate-buffered saline

rhTSH: recombinant human TSH

T4: thyroxine

T3: triiodothyronine

HMVEC: human microvascular endothelial cells

HUVEC: human umbilical vein endothelial cells

BSA: bovine serum albumin

EBM-2: endothelial basal medium 2

CM: conditioned medium

H&E: hematoxilin and eosin

PTU: propylthiouracil

INTRODUCTION

1. Positive correlation between serum TSH level and tumor progression in thyroid cancer patients

Thyroid stimulating hormone (TSH) is well-known for a growth factor of thyrocytes leading TSH-dependent growth of thyroid gland. A number of studies have suggested that high serum TSH concentrations increase likelihood of thyroid cancer in patients presenting with thyroid nodules (1-3). Moreover, higher serum TSH levels have been found associated with aggressiveness and advanced stage of differentiated thyroid cancer (DTC) (4-6). The DTC expresses TSH receptors and usually retains responsiveness to TSH. Suppression of serum TSH concentrations by administering L-T4 may inhibit progression of DTC, which is supported by evidence of improved relapse-free and overall survival (7, 8). Thus, TSH suppression has been used as an important clinical therapeutic tool of patients with DTC, especially in high-risk patients (9-11).

2. Regulatory mechanism of TSH on growth of differentiated thyroid tumor cells

TSH binds with its receptors on the thyrocyte surface and activates two main signal transduction pathways, the adenylate cyclase (AC) /protein kinase A (PKA) pathway and the phospholipase C (PLC) /protein kinase C (PKC) pathway (12, 13). Activation of the AC/PKA pathway by TSH is commonly thought to be involved in differentiation of follicular thyrocytes, whereas PLC/PKC stimulates undiffrentiation and growth of transformed thyrocytes (14). Previous studies reported that TSH stimulates the growth and invasion in differentiated follicular thyroid cancer via PKC activation (15, 16).

3. Vascular endothelial growth factor (VEGF)-regulated angiogenesis in thyroid cancer

The tumor microenvironment is a complex environment, including surrounding blood vessels, immune cells, fibroblasts, bone marrow-derived inflammatory cells, signaling molecules and the extracellular matrix (17). Especially, angiogenesis plays a crucial role in tumor growth, invasion and metastasis. Among several angiogenic growth factors, the vascular endothelial growth factor (VEGF) and its receptors are key inducers of tumor angiogenesis (18, 19). VEGF is a homodimeric glycoprotein that

promotes endothelial cell growth and migration, stimulates the formation of collateral blood vessels, and increases vascular permeability (20). Since 2004, several drugs that target VEGF or its receptors have been approved for the treatment of various malignant diseases. It has been demonstrated that the upregulation of VEGF expression in human thyroid cancer tissues is correlated with incidence, progression, or metastasis of thyroid cancer (21-23).

Therefore, a few *in vitro* experiments were performed to know whether the expressions of VEGF in thyroid cancer cells are affected by TSH signaling, and it was demonstrated that TSH induced VEGF secretion by the TSH receptor-mediated activation of PLC/PKC pathway (24) in thyroid cancer cells (24, 25) as well as in normal human thyroid cells (26) In *in vivo* studies, there is only one report showing TSH stimulated angiogenesis and local VEGF expression in normal mouse thyroid (27), and to the best of our knowledge, there is no *in vivo* study demonstrating the effects of TSH on angiogenesis-related tumor growth in thyroid cancer. As a human study, a positive correlation between preoperative serum TSH level and tumor VEGF protein expression was observed (28), although it failed to demonstrate a relationship of TSH or VEGF with tumor size or the TNM stage (28). The *in*

vivo effect of TSH-stimulated VEGF on tumor vasculature and its effects on tumor growth in thyroid cancer still remain to be elucidated.

4. Tumor-associated macrophage (TAM) in thyroid cancer

Among the components of tumor microenvironment, the innate and adaptive immune cells have been recently proposed (29). Among them, macrophages are particularly abundant and play protumoral and immunosuppressive roles. Tumor-associated macrophages (TAMs), macrophages presenting in the tumor microenvironment, promote tumor cell proliferation and angiogenesis (30). Moreover, several reports have suggested that TAMs are associated with disease progression and poor prognosis in some human cancers including thyroid cancer (31-33). Previous studies demonstrated that a high TAM density is present in poorly differentiated thyroid cancer (34) and is correlated with larger tumor size (33) and advanced TNM stage (35) in papillary thyroid cancer. However, a relationship of TSH and TAM has not been elucidated.

5. Aims of Study

We hypothesized that TSH induces the growth of DTC by changing tumor microenvironment, specifically through stimulating angiogenesis or activating macrophages. Thus, using mouse tumor models as well as *in vitro* cell lines, we investigate the functional effect of TSH on tumor growth and its mechanisms related to tumor microenvironment focused on angiogenesis and activation of macrophages.

MATERIALS AND METHODS

1. Mice

Five-week-old female BALB/c nu/nu mice (mean body weight 17.8 ± 0.9 g) were purchased from Orient Bio Inc. (Sungnam, South Korea) and housed in the specific pathogen-free facility under automatically controlled airconditions of temperature (21 ± 2°C), humidity (about 50 ± 5%), and lighting (12:12-h light-dark cycle). The mice were fed commercial pelleted chow (AIN-76A rodent purified diet, Orient Bio Inc., Sungnam, South Korea) and tap water *ad libitum*. All mice were sacrificed by CO2 anesthesia. Our Institutional Animal Care and Use Committee approved the protocols for the animal study (No. SNU-141224-2), and all animals were maintained and used in accordance with the Guidelines for the Care and Use of Laboratory Animals of the Institute of Laboratory Animal Resources, Seoul National University.

2. Cell cultures

A tumorigenic clone of the BHP10-3 cell line, BHP10-3SC, human RET/PTC1-mutated papillary thyroid cancer cell line, was developed and

kindly provided by doctors Gary L. Clayman (MD Anderson Cancer Center, Houston, TX, USA) and Soon-Hyun Ahn (Seoul National University, Seoul, Korea) (36, 37). The human anaplastic thyroid carcinoma cell line, FRO was kindly provided from Dr. Minho Shong (Chungnam National University College of Medicine, Daejeon, Korea) (38). Both cell lines were maintained at 37°C in a humidified 5% CO2 atmosphere in Roswell Park Memorial Institute (RPMI) 1640 with 10% fetal bovine serum (FBS). Human microvascular endothelial cells (HMVEC) were purchased from Cascade biologics, inc. (Portland, OR, USA) and human umbilical vein endothelial cells (HUVEC) were kindly provided by Dr. HS Kim (Seoul National University College of Medicine, Seoul, Korea). HMVEC and HUVEC cells which represent human microvascular and macrovascular endothelial cells, respectively, were cultured in 0.5% bovine serum albumin (BSA)/endothelial basal medium 2 (EBM-2) medium. All cell lines were tested and found to be free of mycoplasma by culture and by DNA staining. Cell line authentication was achieved by genetic profiling using short tandem repeat (STR) analysis.

For injection into nude mice, cultured cells were removed from culture dishes using trypsin/EDTA and were washed and resuspended in phosphate-buffered saline (PBS) without Ca 2+ or Mg 2+. Cell clumps were dissociated

by gentle pipetting with a Pasteur pipette. Cell concentration and viability were determined using 0.06% trypan blue, and 5×10^6 cells were injected subcutaneously through 29-gauge needles at both scapular areas of 7-week-old BALB/c nu/nu mice.

For *in vitro* assay, BHP10-3SC and FRO cells were cultured at a density of 10^5 cells into 12-well plates and incubated with recombinant human TSH (rhTSH) at a concentration of 0, 2 and 20 ng/μl for indicated times.

3. Experimental protocols of TSH treatment on mouse tumor model

As for the first study to know the effects of TSH with different duration of treatment, 6 mice were divided into the 5- (n = 2), 14-day (n = 1) administration of rhTSH, and control (n = 3) groups. BHP10-SC cells were used for xenografts. The thyroid stimulatory effect of rhTSH has been well studied in the mouse (27, 39), and the supra-physiologic dose (1.5 μg/g/day) of rhTSH (Thyrogen®, Genzyme Therapeutics, Cambridge, MA) or normal saline (NaCl 0.9%) was daily administrated intraperitoneally for the indicated duration (Figure 1A).

From results of the pilot study, we could determine the 14-day treatment is

better to observe the changes of tumor vasculature than the 5-day treatment. For the second experiment, 10 mice were used for the experiment and divided into the treated (n = 5) and control (n = 5) groups. When the greater diameter of tumor became 5 mm or larger, treatment was initiated. rhTSH (1.5 μg/g) delivered intraperitoneally for 15 days in the treated group and the same volume of normal saline was injected intraperitoneally for the same duration in control group.

Since there were wide variations in the tumor size within the same group, we evaluated tumorigenicity of the cell line, and found the effects of cell passages. Therefore, the BHP10-3SC cells of earlier passage (15th passage) were used in the third experiment for reducing the values of standard deviation. Total of 20 mice were divided into 2 weight-matched groups: rhTSH (n = 10) and control (n = 10) groups. At 5 days after tumor cell injection, when tumor sizes of all visible tumors were 5mm or larger in their greater diameter, treatment was initiated. rhTSH (1.5 μg/g) and normal saline were injected to the mice intraperitoneally for 15 days. Tumor size was measured every 3 days. On the indicated days after the treatments, mice were sacrificed by CO2 anesthesia. FITC-labeled SiO2 nanoparticles was injected to two mice of each group via the tail vein shortly before sacrificing

them (Figure 1B). Tumors were cut longitudinally to provide a representative fragment for histologic analyses, and then fixed in 4% paraformaldehyde. A tiny portion (~ 1 mm^3) of the tumor was fixed in 2.5% glutaraldehyde (Ted Pella, Redding, CA, USA) for electron microscopy, and the remainder was frozen in liquid N2 for subsequent protein or RNA isolation.

(A)

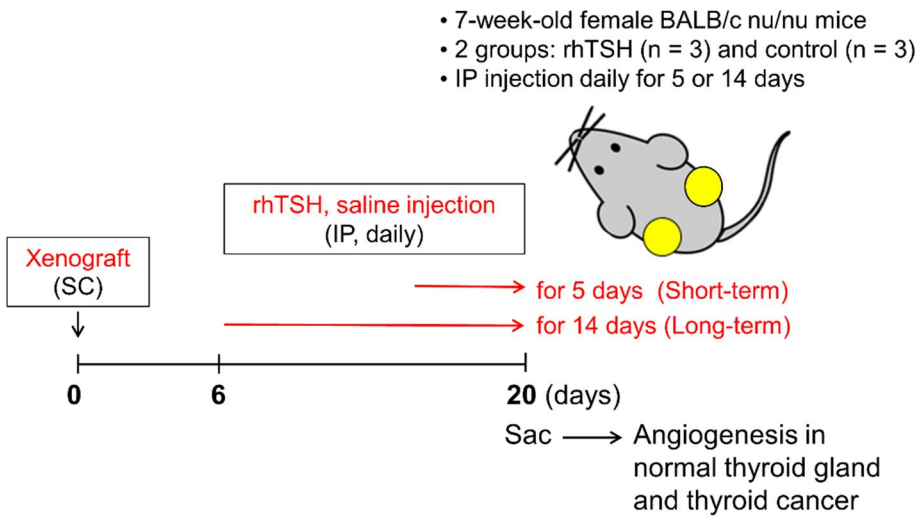

(B)

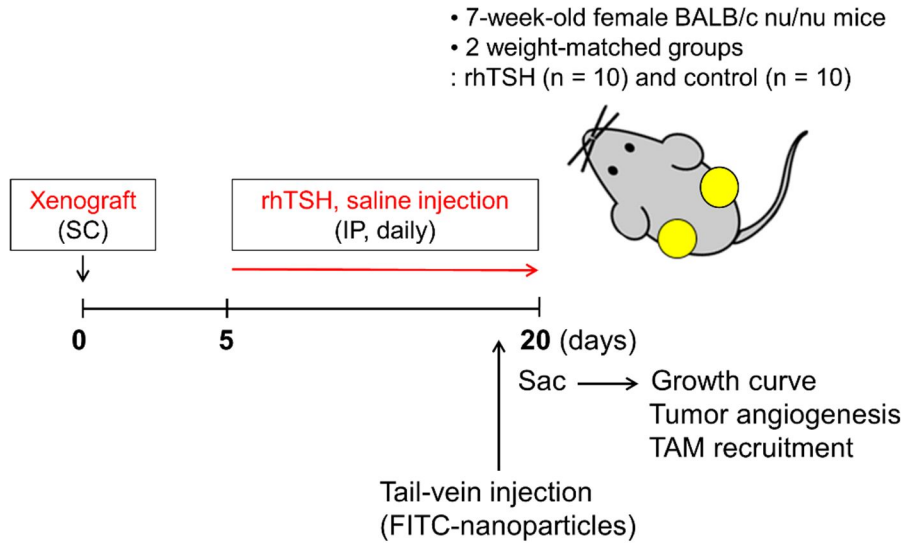

Figure 1. Schematic diagram of the experimental protocol.

(A) The experimental protocol of the pilot (first) study. The BHP10-3SC cells (5×10^6) were injected subcutaneously at both scapular areas of BALB/c nu/nu mice. rhTSH (1.5 μg/g) and normal saline were administered intraperitoneally to the mice for 5 or 14 days. All mice were sacrificed and

their tissue samples were analyzed at the same time.

(B) The experimental protocol of the main (second and third) studies. The BHP10-3SC cells (5×10^6; 17th and 15th passage for the second and third experiments, respectively) were injected subcutaneously at both scapular areas of BALB/c nu/nu mice. Total of 20 mice were divided into 2 weight-matched groups: rhTSH (n = 5 and 10 for the second and third experiments, respectively) and control (n = 5 and 10 for the second and third experiments, respectively) groups. At 5 days after tumor cell injection, when visible tumors began to appear, treatment was initiated. rhTSH (1.5 μg/g) and normal saline were injected to the mice intraperitoneally for 15 days. Shortly before sacrificing mice, we injected FITC-labeled SiO2 nanoparticles into the tail vein.

4. Measurement of tumor size

In order to determine tumor volume by external caliper, the greatest longitudinal diameter (length) and the greatest transverse diameter (width) were measured (Figure 2). Tumor volume based on caliper measurements were calculated by the modified ellipsoidal formula: Tumor volume = $1/2(\text{length} \times \text{width}^2)$ (40).

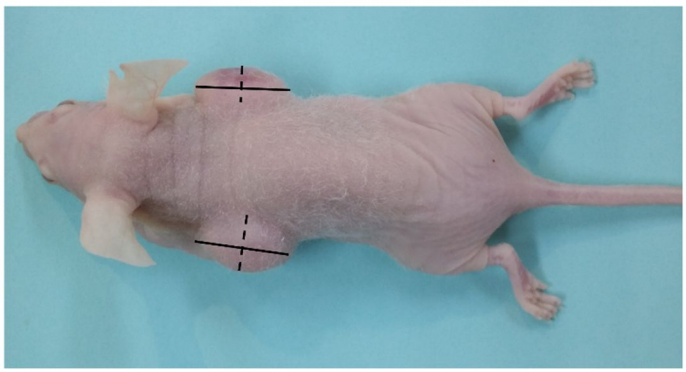

Figure 2. Athymic nude mice with tumors of BHP10-3SC (15th passage). Tumors grew symmetrically on both scapular areas of mice. To determine tumor volume, the greatest longitudinal diameter (solid line) and the greatest transverse diameter (dotted line) were measured by a caliper.

5. Measurement of serum thyroid hormone

Serum free thyroxine (T4) and triiodothyronine (T3) concentrations were measured by coated tubes radioimmunoassays (DPC, Diagnostic Products, Los Angeles, CA, USA).

6. Immunofluorescence, H&E, and immunohistochemistry

For the staining, tumors and thyroid glands fixed in 4% paraformaldehyde were embedded with tissue freezing medium (Leica Instruments, Nussloch, Germany) or paraffin, and sectioned. For the immunofluorescence staining, samples were blocked with 5% goat serum in PBST (0.1% Triton X-100 in PBS) and incubated for 3 hr at room temperature with the following primary antibodies: anti-CD31 (hamster, clone 2H8, Millipore, Billerica, MA, USA), and anti-VEGF-A (goat polyclonal, R&D Systems, Minneapolis, MN, USA). After several washes with PBS, sections were incubated for 2 hr at room temperature with one or more of the following secondary antibodies: Cy3- or FITC- conjugated anti-hamster IgG (Jackson ImmunoResearch, West Grove, PA, USA), and Cy3- or FITC-conjugated anti-goat IgG (Jackson ImmunoResearch, West Grove, PA, USA). Nuclei were stained with 4',6-diamidino-2-phenylindole (DAPI, Invitrogen, Carlsbad, CA, USA). Zeiss

LSM 510 confocal microscope equipped with argon and helium-neon lasers (Carl Zeiss, Jena, Germany) was used to visualize the fluorescent signals and to obtain digital images.

To verify the changes of vascular permeability, FITC-labeled SiO2 nanoparticles (80 nm in diameter) were developed and kindly provided by Dr. Youngeun Kwon (Dongguk University, Seoul, Korea). Shortly after injecting FITC-labeled nanoparticles into the mice via their tail vein, we extracted the tumors and observed them by a fluorescence microscope (Carl Zeiss, Jena, Germany) at ×100 magnification.

Paraffin-sectioned tissues were stained with hematoxilin and eosin (H&E) or had immunohistochemistry performed using the antibodies to CD31 and F4/80. The H&E and immunohistochemistry images were captured by a microscope equipped with CCD camera (Carl Zeiss, Jena, Germany).

7. Electron microscopy

Tissues for transmission electron microscopy fixed with 2.5% glutaraldehyde (Ted Pella, Redding, CA, USA) in PBS overnight and washed 5 times with cacodylate buffer (0.1 M) containing 0.1% CaCl2. Tissues were post-fixed for 2 hr with 1% OsO4 in 0.1 M cacodylate buffer

(pH 7.2) and washed in cold distilled water. Tissue dehydration was conducted with ethanol series and propylene oxide, and the tissues were embedded in Embed-812 (EMS, Fort Washington, PA, USA). Following resin polymerization for 36 hr, the tissues were serially sectioned using an ULTRACUT UC7 ultramicrotome (Leica, Austria) and mounted on formvar-coated slot grid. After staining with 4% uranyl acetate and lead citrate, the sections were observed using a Tecnai G2 Spirit Twin transmission electron microscope (FEI, Eindhoven, Netherlands).

8. RNA extraction and real time-PCR analysis

Total RNA from fresh frozen tissues or cultured cells was extracted using TRIzol Reagent (Invitrogen, Carlsbad, CA, USA). The real time-PCR was performed by using a Perkin-Elmer GeneAmp PCR System 9600 (Waltham, MA, USA). Primers for the real-time PCR are as follows: VEGF-A, forward 5'-ACGAACGTACTTGCAGATGTGAC-3' and reverse 5'-GCGGCAGCGTGGTTTCTGTA-3'; VEGFR2, forward 5'-ACCAGAAGTAAAAGTGATCCCAGA-3' and reverse 5'-TCCACCAAAAGATGGAGATAATTT-3'; β-actin, forward 5'-GCTCTTTTCCAGCCTTCCTT-3' and reverse 5'-

CTTCTGCATCCTGTCAGCAA-3'. Results presented the average of three experiments.

9. Conditioned medium of TSH-treated BHP10-SC cells

BHP10-SC cells cultured in RPMI-1640 medium supplemented with 10% FBS were treated with TSH (20 ng/μl) or saline. The cells were seeded on 100 mm culture dishes with 3×10^5 cells/ml in 10 ml of medium. After 24 and 72 h, the media were harvested, filtered, and stored at −70 ºC. Conditioned media from TSH-treated and saline-treated BHP10-3 cells were called TSH-CM and control-CM, respectively.

10. Measurement of VEGF-A protein levels

The protein levels of VEGF-A in TSH- or control-CM were determined using ELISA assays (R&D Systems, Minneapolis, MN, USA). Samples were tested in duplicate.

11. Cell migration and tube formation assay

To evaluate cell migration potential, the transwell migration assay was performed. BHP10-3SC cells were treated with TSH (20 ng/μl) or saline for

24 h. HMVEC and HUVEC cultured in 0.5% BSA/ EBM-2 medium were treated with TSH- or control-CM (1:1 dilution). The 8 μm pore-size polycarbonate membrane (Corning, NY, USA) was pre-coated with gelatin and the inserts were placed into a 24 well plate. The upper and lower chambers were plated with HMVEC or HUVEC cells and TSH- or control-CM, respectively. After 4 h, non-migrating cells were removed from the surface of the upper membrane with a cotton-tipped applicator and the inserts were stained with 1% crystal violet solutions. For tube formation assay, HMVEC and HUVEC cells were cultured in Matrigel-coated plate for 3 h with 0.5% BSA/EBM-2 medium and TSH- or control-CM (1:1 dilution). The tube-like structures were observed and photographed by microscopes at ×40 magnification.

12. Morphometric analysis

Morphometric analyses of thyroid glands, tumor vessels, cell migration, and tube formation were performed using ImageJ software (http://rsb.info.nih.gov/ij). Heights of thyroid follicular cells were averaged among 10 consecutive thyrocytes in H&E-stained images. For vascular densities, CD31+ or FITC+ area was measured in 4 random 0.05 mm^2 areas

and presented as a percentage of the total measured area. Vascular diameters were averaged among 10 consecutive blood vessels in 3 random 0.05 mm^2 areas. Numbers of fenestrae in 10 μm vessel perimeter of the capillary ECs were measured on 10 random areas of TEM images. TAMs were scored by the number of F4/80+ cells/total tumor cells under ×400 magnification. The density of migrated cells and the number of maturated tubes were measured in three randomly selected fields per well (×100).

13. Statistical analysis

Statistical comparisons used Mann-Whitney test or 2-tailed Student's t test for two groups or Kruskal-Wallis test with Bonferroni correction for three groups. Statistical significance was defined as two-sided *P* values <0.05.

RESULTS

1. Time effects of TSH on angiogenesis in normal thyroid and thyroid cancer

1) Effects of TSH on thyrocytes and angiogenesis in thyroid gland

To evaluate whether the dose and duration of rhTSH administration were adequate, we observed the rhTSH-induced structural changes in thyroid glands. The size of both thyroid lobes and thyroid follicles was increased by the administration of rhTSH, especially in the 14-day treatment group. The mean height of follicular cells in control, 5-, and 14-day treatment of rhTSH groups was 3.9 ± 0.6, 7.7 ± 2.0, and 14.2 ± 2.2 μm, respectively (P <0.001; Figure 3). The VEGF-A was expressed along thyroid follicular area and it was surrounded by perifollicular capillaries (Figure 4). The vascular structure of perifollicular capillaries was more prominent and enlarged in rhTSH group relative to control (10.6 ± 0.9 vs. 4.0 ± 0.2 μm in vascular diameter, P <0.001), although there was no change in the vascular density (Figure 4). The thyroid gland capillaries have diaphragm-covered fenestrations which are critical in maintaining vascular permeability for low molecular weight hydrophilic molecules transport. Therefore, we next

questioned whether the modulation of TSH receptor signaling can alter the ultrastructure of the discontinuous, fenestrated endothelium in thyroid glands. Administration of rhTSH for 14 days increased the number of endothelial fenestrae, compared with control (19.2 ± 2.5 vs. 6.0 ± 1.9 per 10 μm vessel perimeter, $P = 0.001$; Figure 5).

2) Effects of TSH on angiogenesis in thyroid cancer

The histologic findings of tumors were consistent with papillary thyroid cancer and not different among groups. Since the immunofluorescence staining using mouse VEGF-A antibody was failed, we could not evaluate VEGF-A expression in all tumor samples. The vascular density in peripheral area of tumors was significantly increased in rhTSH groups than control (12.3 ± 0.7% vs. 5.7 ± 0.8%, $P = 0.004$). In particular, we could find more tortuous and dilated vessels in tumors of long-term rhTSH treatment (23.0 ± 1.7 μm in vascular diameter) than those of short-term treatment (9.5 ± 0.8 μm) or control (7.4 ± 0.5 μm) ($P < 0.001$, respectively; Figure 6). We did not observed endothelial fenestrae in tumor tissues.

From those results, we decided to treat rhTSH for 14 days to investigate the effects of rhTSH on thyroid cancer.

(A)

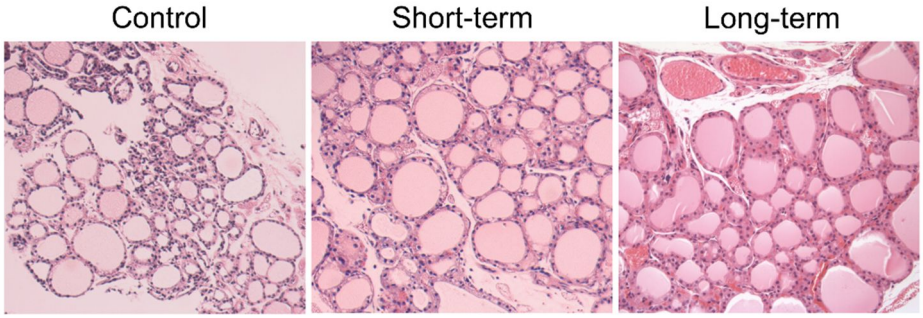

(B)

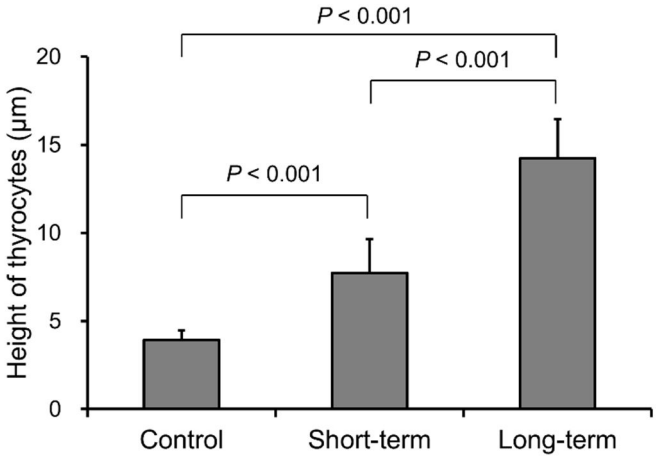

Figure 3. Effects of TSH on follicular remodeling in thyroid glands.

(A) Images of H&E stained follicular cells in thyroid glands of control (n = 3), short-term (n = 2), and long-term (n = 1) treatment of rhTSH groups. Short-term, for 5 days; Long-term, for 14 days (H&E, ×400).

(B) Comparisons of the heights of follicular cells in control, short-term, and long-term treatment of rhTSH groups. Heights of thyroid follicular cells were averaged among 10 consecutive thyrocytes in H&E-stained images. Data were shown as mean ± standard error.

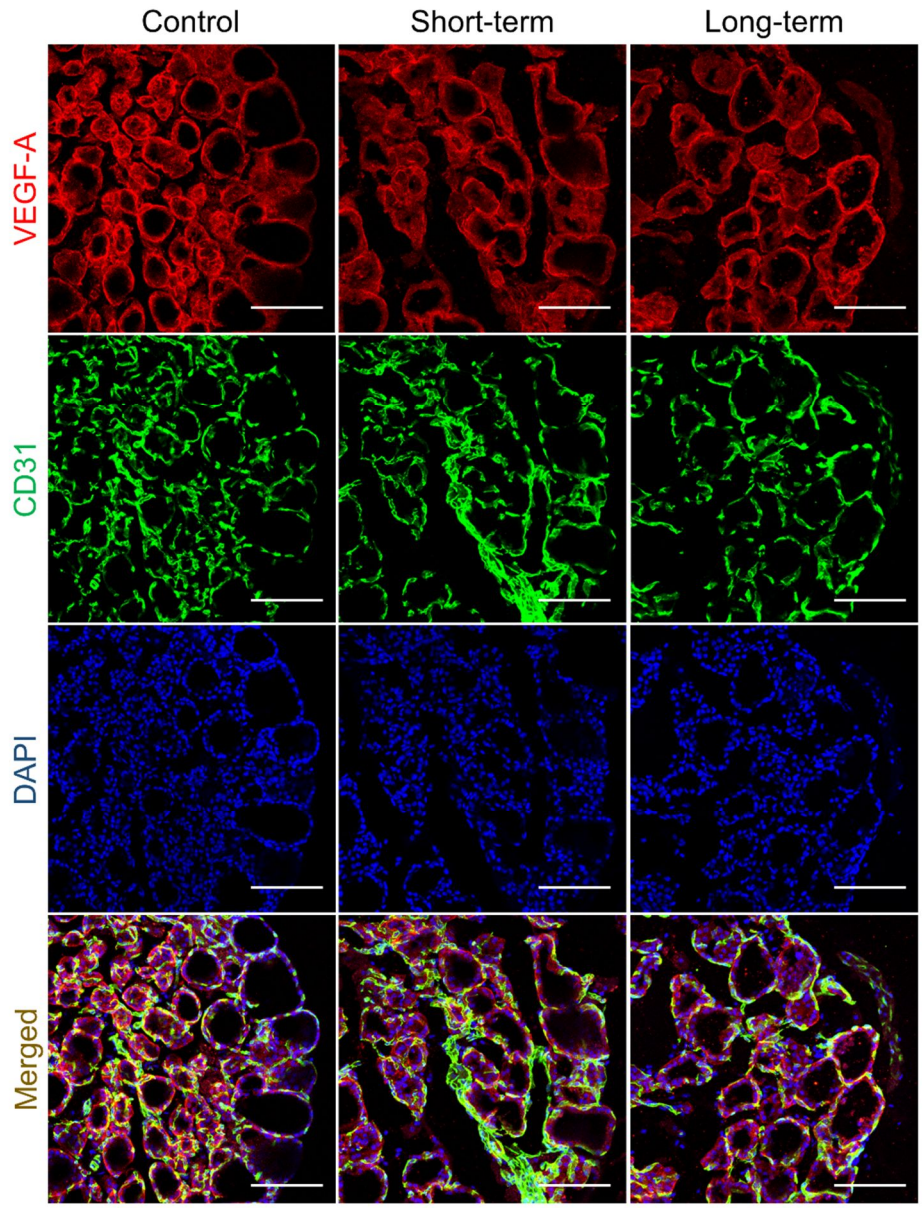

Figure 4. Effects of TSH on vascular remodeling in thyroid glands.

Images of immunofluorescence staining for VEGF-A (red), CD31 (green), and DAPI (blue). Control (left), 5- (middle), and 14-day treatment (right) groups. Scale bars, 100μm.

(A)

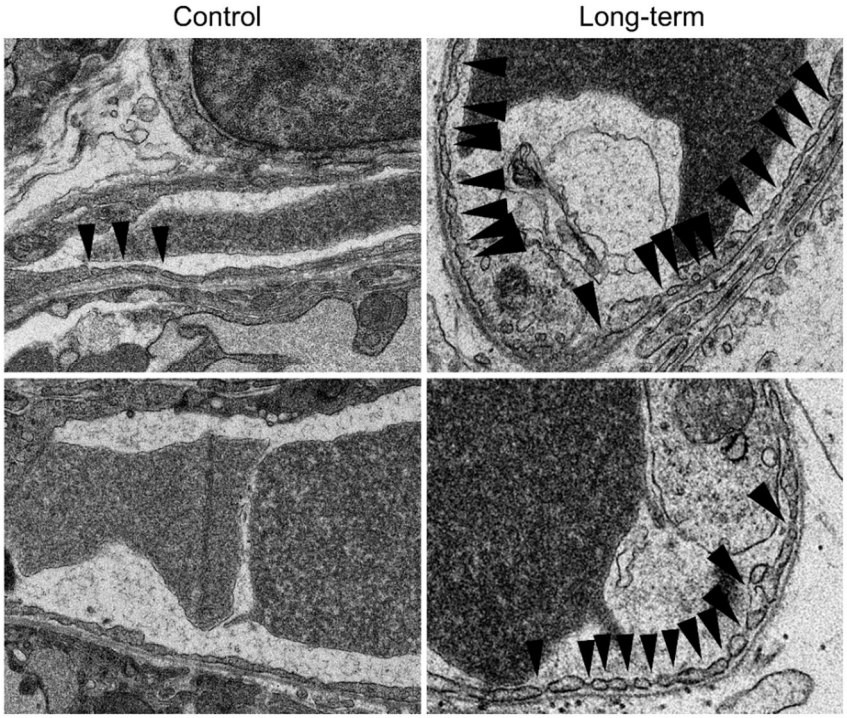

(B)

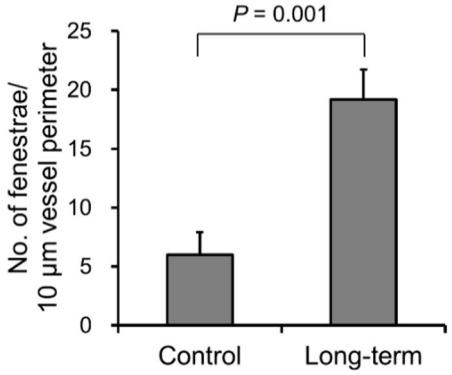

Figure 5. Effects of TSH on endothelial fenestrae in thyroid glands.

(A) Transmission electron microscopic findings showing the interface between endothelial cells and follicular cells in thyroid glands of control (left) and 14-day treatment (right) groups. Arrowheads indicate endothelial fenestrae. (B) Comparison of the number of endothelial fenestrae per 10 μm vessel perimeter on 10 random areas of TEM images of control and 14-day treatment mice. Data were shown as mean ± standard error.

(A)

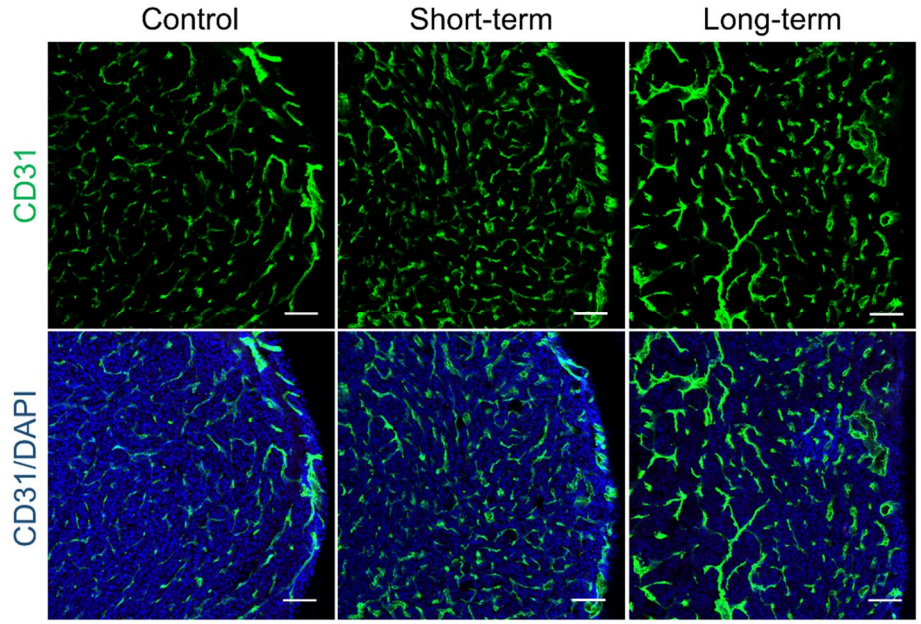

(B)

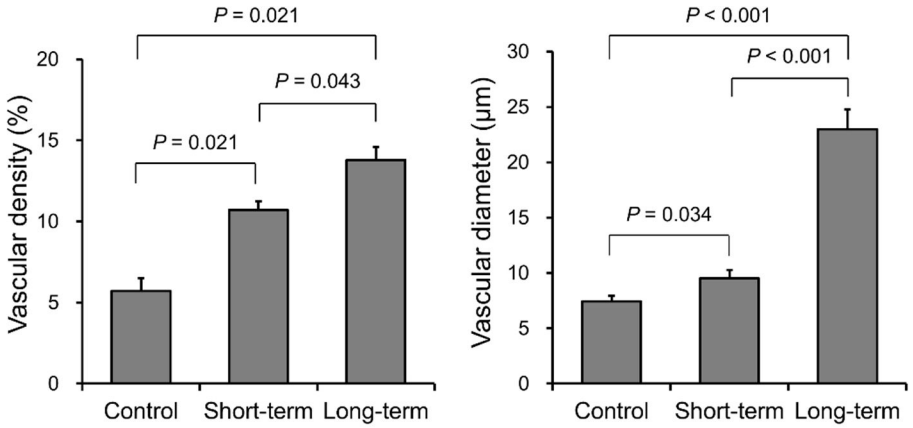

Figure 6. Effects of TSH on vascular remodeling in thyroid cancers.

(A) Images of CD31-positive blood vessels in thyroid cancer tissues of control and rhTSH groups. Short-term, for 5 days; Long-term, for 14 days. Scale bars, 100μm. (B) Comparisons of the CD31+ vascular density (%) and vascular diameter averaged among 10 consecutive blood vessels in control, short-term, and long-term treatment of rhTSH groups. Data were shown as mean ± standard error.

2. Effects of TSH on tumor growth

1) Effects of cell passages on tumorigenesis of xenografts

Administration of 1.5 μg/g/day of rhTSH for 15 days significantly increased serum free T4 and T3 level (1.04 ± 0.42 and 0.67 ± 0.16 ng/ml, respectively) compared with control (0.40 ± 0.10 and 0.25 ± 0.01 ng/ml, respectively). Tumors in rhTSH-administrated group showed a trend of rapid growth relative to control group, but there was no statistically significant difference in tumor volume between groups (at 15 days after treatment, $P = 0.833$; Figures 7 and 8). There were wide variations in tumor size within the same group, which made large standard deviation. Moreover, 5 of 20 xenografts could not form the tumors till the end of experiment. Therefore, we found out that the evaluation of the tumorigenicity of BHP10-3SC cell line would be needed.

(A)

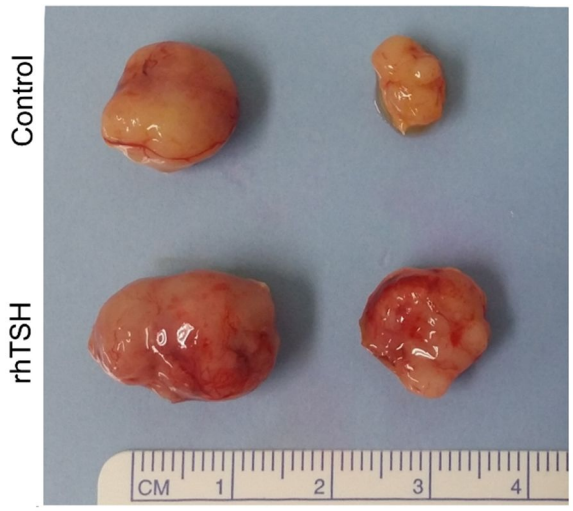

(B)

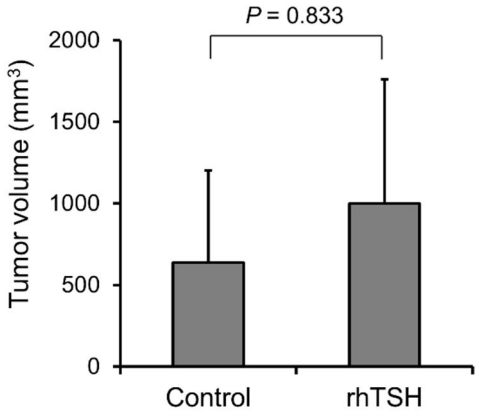

Figure 7. Gross images of BHP10-3SC tumors (17th passage) in control and rhTSH groups.

(A) rhTSH (1.5 μg/g) delivered intraperitoneally for 15 days in the treated group and the same volume of normal saline was injected intraperitoneally for the same duration in control group. Tumors in rhTSH group were bigger and hypervascular than those in control group. (B) Comparison of final tumor volume between control and rhTSH groups. Each group, n = 5.

(A)

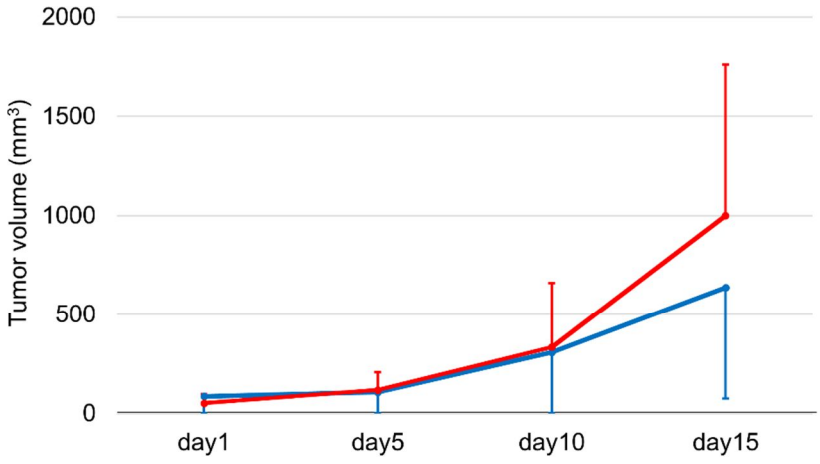

	day1	day5	day10	day15
Control	86.5±97.9	107.0±119.5	308.3±336.7	637.2±563.1
rhTSH	52.6±44.3	118.9±90.7	334.6±326.0	998.9±761.4
P-value*	0.724	0.724	1.000	0.833

(B)

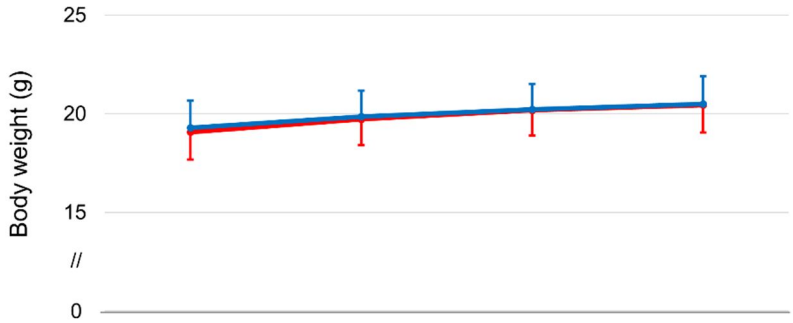

	day1	day5	day10	day15
Control	19.3±1.3	19.9±1.2	20.2±1.1	20.5±1.4
rhTSH	19.1±1.4	19.7±1.3	20.2±1.3	20.5±1.4

Figure 8. Growth curves of BHP10-3SC (17th passage) cell xenografts.

(A) Xenografts grew quickly in rhTSH group, but there was no statistically significant difference between rhTSH and control groups. Data were presented as mean ± standard deviation. **P* value for comparison between control and rhTSH groups at the point of measurement. (B) There was no difference in the average body weight between the two groups.

Considering the possibility of evolutionary changes which occurred by the continual subculture of this cell line, we used cells of the earlier passage (5th passage) than those of the previous passage (17th passage) after primary culture and transplanted the same volume of the cells to nude mice. Tumors were formed and grew much more rapidly compared to those of the previous cell line, but tumor shape and size was relatively consistent. The greatest longitudinal diameter of tumors ranged from 7.0 to 11.7 mm at 5 days after xenografts, and nude mice were euthanized after 17 days because the tumors grew over 20.0 mm. Although STR profiles were the same with the original cell line of BHP10-3SC, growth rate and consistency of the tumors were different. We found that tumors grow fast as the passage of cell line is earlier and tried to select the cell line with adequate growth rate and consistent growth properties. Therefore, we could decide the ideal passage and number of cells: 5×10^6 of BHP10-3SC cells with 15th passage after primary culture.

2) Effects of TSH on tumor growth

In the next experiment with the cells of 15th passage, the shape and size of tumors were more even within the same group than those in the previous experiment. Additionally, there was a significant difference in the tumor

volume between control and rhTSH groups (on day 10, $P = 0.004$; day 13, $P = 0.008$; day 15, $P = 0.010$) (Figures 9 and 10). In particular, the tumor bleeding was observed in 3 of 10 mice of rhTSH group, but not in those of control group (Figure 11). The tumor hemorrhage occurred from day 14 of treatment, and it would be caused by rapid expansion of tumor and abnormal tumor vessels. Histologic findings of the tumors in both groups were consistent with differentiated papillary thyroid cancer and rarely had necrotic portions (Figure 12).

(A)

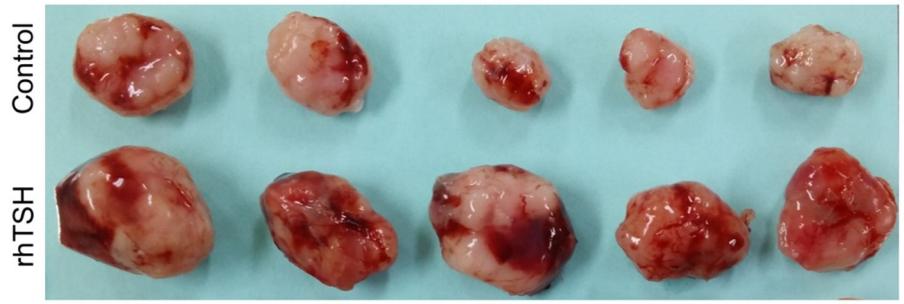

(B)

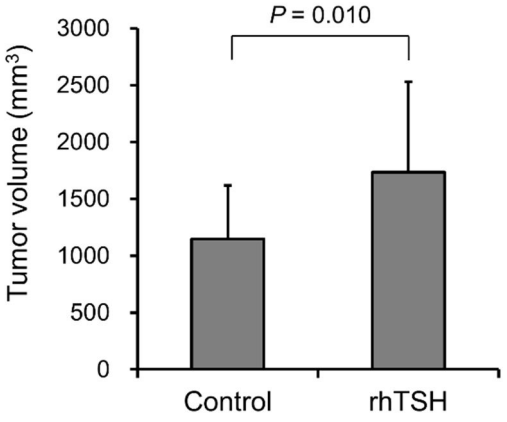

Figure 9. Gross images of BHP10-3SC tumors (15th passage) in control and rhTSH groups.

(A) At 5 days after tumor cell injection, when visible tumors began to appear, treatment with rhTSH was initiated. rhTSH (1.5 μg/g) and normal saline were injected to the mice intraperitoneally for 15 days. Tumors in rhTSH group were bigger, more hypervascular and hemorrhagic than those in control group. (B) Comparison of final tumor volume between control and rhTSH groups. Each group, n = 10.

(A)

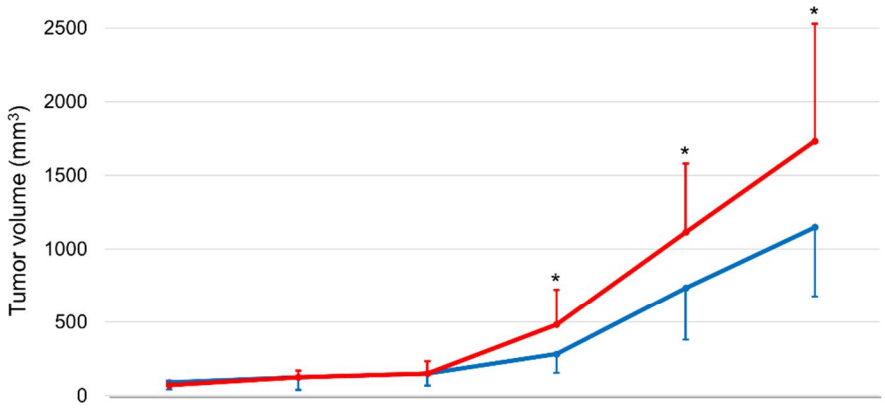

	day1	day4	day7	day10	day13	day15
Control	89.9±48.4	125.2±85.1	150.9±83.6	282.4±126.5	734.4±354.6	1148.8±471.1
rhTSH	72.0±30.8	124.9±43.5	151.0±81.9	484.8±238.4	1114.6±465.8	1733.4±793.5
P-value**	0.191	0.992	0.998	0.004	0.008	0.010

(B)

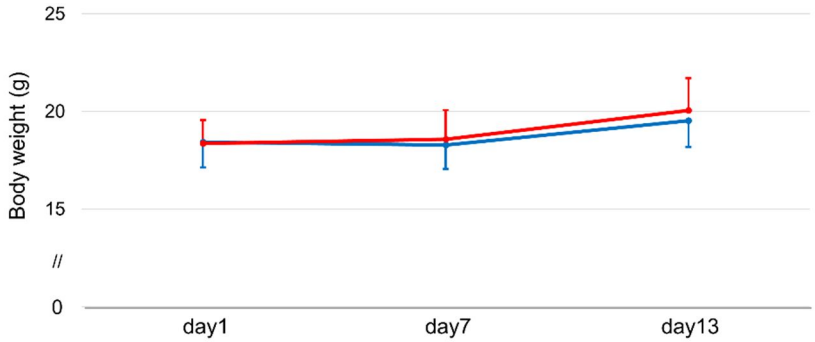

	day1	day7	day13
Control	18.4±1.3	18.3±1.2	19.5±1.3
rhTSH	18.4±1.2	18.6±1.5	20.1±1.7

Figure 10. Growth curves of BHP10-3SC (15th passage) cell xenografts.
(A) Xenografts grew quickly in rhTSH group, and there was a significant difference in the tumor volume with control group. *P <0.05. Data were presented as mean ± standard deviation. **P value for comparison between control and rhTSH groups at the point of measurement. (B) There was no difference in the average body weight between the two groups.

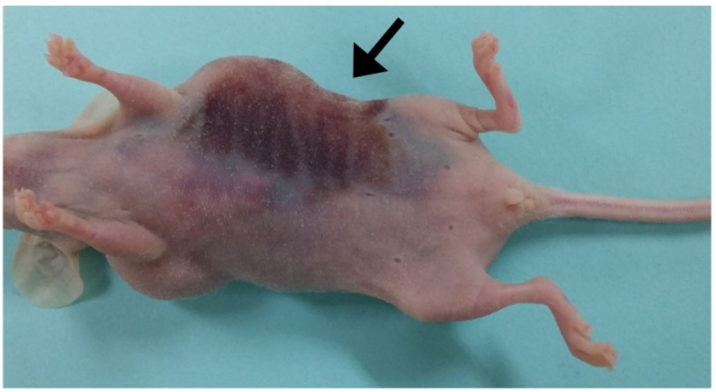

Figure 11. Tumor bleeding observed in the mice of rhTSH group.

Unlike the mice of control group, tumor bleeding around their tumors occurred in 3 of 10 mice of rhTSH group. The arrow indicate the hemorrhage from tumor vessels.

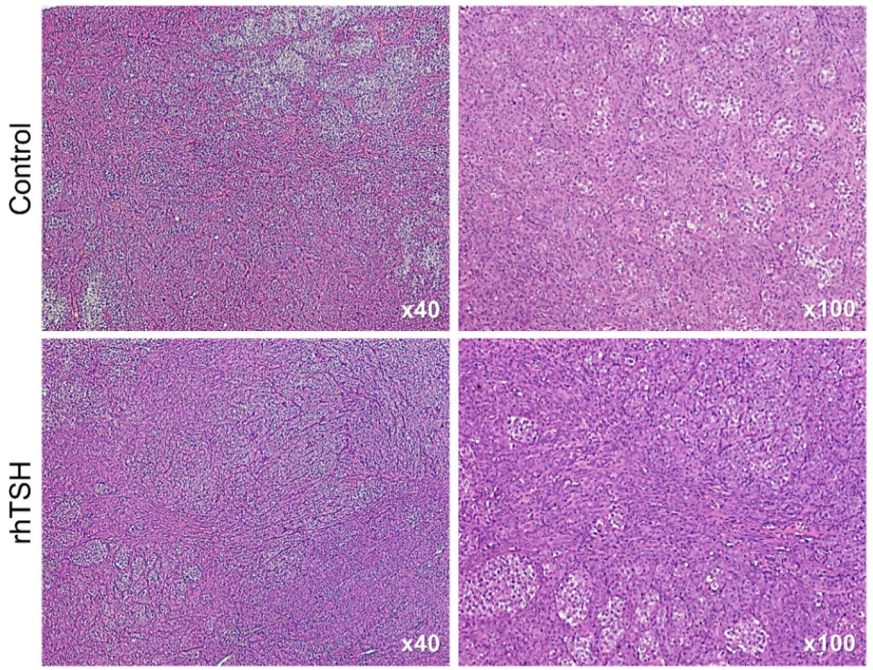

Figure 12. Histologic features of thyroid cancer tissues.

Images of H&E stained thyroid cancer tissues of control and rhTSH-treated mice (left, ×40; right, ×100). Tumors were extracted and analyzed after 15 day-treatment of rhTSH or saline.

3. In vivo effects of TSH on angiogenesis

1) Angiogenesis and vascular permeability

Because tumors in rhTSH group were more hypervascular and hemorrhagic in gross finding (Figures 7 and 9), FITC-labeled SiO2 nanoparticles (80 nm in diameter) were used to verify the changes of vascular permeability. The distribution of nanoparticles in ectopic tumors was along with tumor vasculature. Tumor vascular structure of control group presented relatively reticular and regular pattern, but vessels of rhTSH group spread out with more heterogeneous and irregular pattern. Furthermore, the density of fluorescent nanoparticle in rhTSH group was denser compared with control group (28.5 ± 2.4% vs. 9.1 ± 2.3%, $P = 0.001$; Figure 13). However, those findings were difficult to distinguish the real increase in vascular permeability from the increase in vascular density or diameter (Figure 13).

2) Endothelial fenestration

Considering that endothelial fenestration was increased by TSH stimulation in thyroid glands, we hypothesized that the endothelial structural changes would be induced by TSH receptor activation in DTC. However, it was difficult to evaluate whether the endothelial fenestrae and caveolae were increased, because the tumor vessels formed the heterogeneous and

abnormal vascular network, although several tumor vessels of rhTSH group had the endothelial fenestrae (Figure 14). Tumor microvasculature showed disorganization and lack of the conventional hierarchy of blood vessels unlike the microvasculature of normal tissue such as thyroid gland.

3) VEGF expression

We investigated how vascular remodeling is regulated by a key angiogenic growth factor, VEGF-A, and its receptor during circulating TSH modulations. Immunohistochemistry for VEGF-A and VEGF-R2 was failed to identify their expression, so we examined mRNA expression of them. Quantitative real-time PCR analyses revealed that mRNA expression of VEGF-A (h) and VEGF-R2 (m) was 1.3- and 1.2-fold higher in rhTSH group than control, but there was no significant difference between groups (P = 0.573 and 0.515, respectively; Figure 15).

(A)

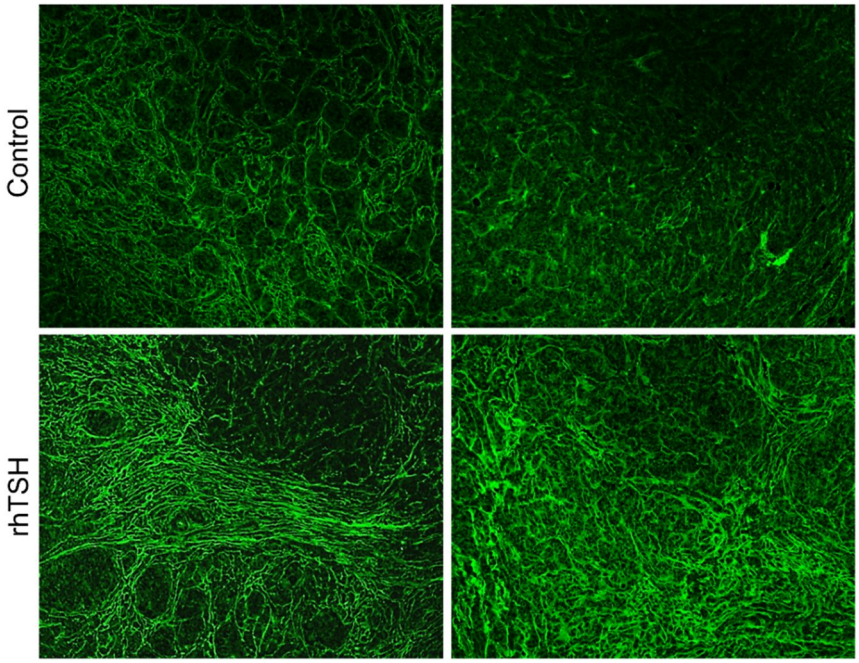

(B)

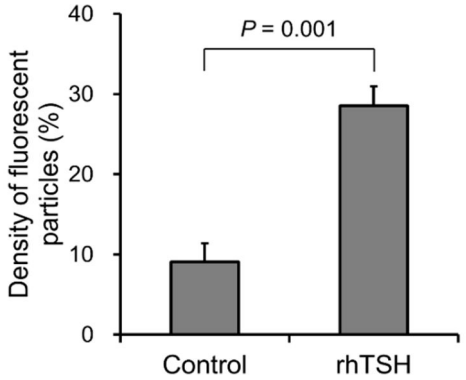

Figure 13. Effects of TSH on angiogenesis and vascular permeability in thyroid cancers.

(A) Shortly before sacrificing mice, FITC-labeled SiO2 nanoparticles (80 nm in diameter) were injected into the tail vein. The distribution of nanoparticles in the tumors was along with tumor vessels. The density of fluorescent particles was increased in rhTSH group (IF, × 100). (B) Comparison of FITC+ density (%) measured in 4 random areas between control and rhTSH groups. Each group, n = 2.

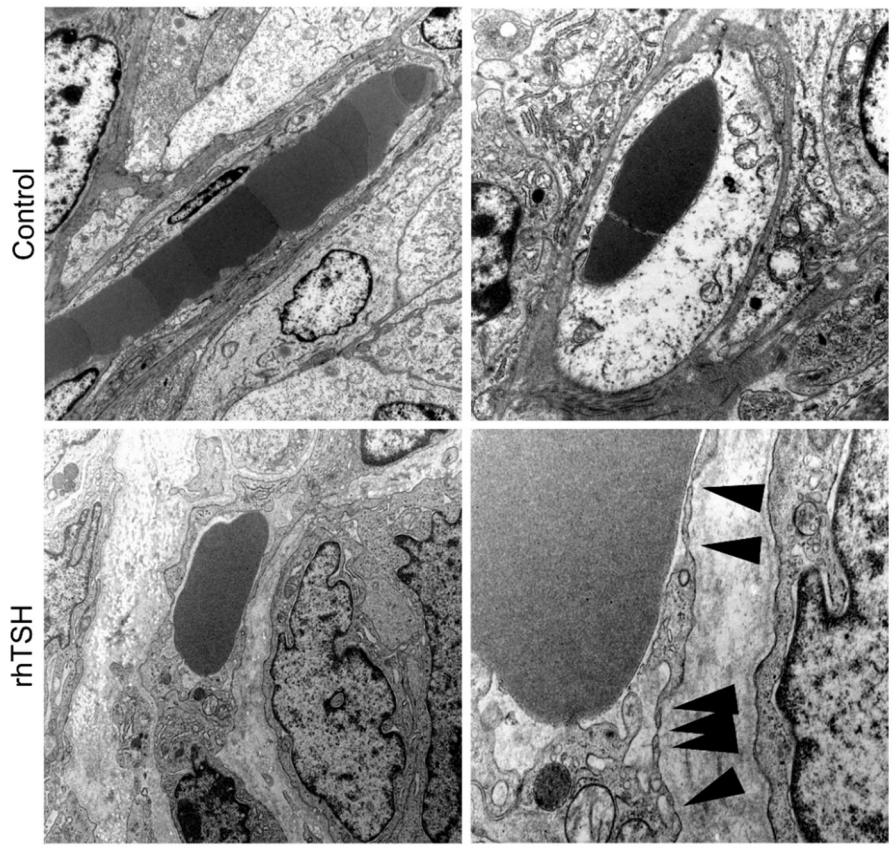

Figure 14. Effects of TSH on endothelial fenestrae in thyroid cancers.

The endothelial fenestrae (arrowheads) were observed in several tumor vessels of rhTSH group, but the tumor vasculatures of both groups were heterogeneous and abnormal.

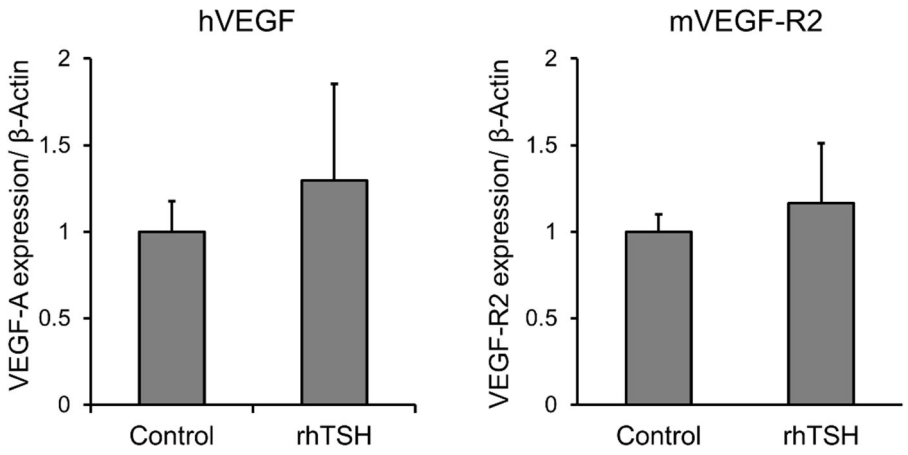

Figure 15. Effects of TSH on the expression of thyroid cancer-derived VEGF-A and endothelial VEGF-R2 in thyroid cancer tissues.

Expressions of VEGF-A and VEGF-R2 genes were higher in rhTSH group, but the differences were not statistically significant (P = 0.573 and 0.515, respectively). Each group, n = 10.

4. In vivo effects of TSH on TAM

Circulating monocytes and macrophages are actively recruited into tumors during tumor progression. We postulated TAM recruitment could be promoted as abnormal tumor angiogenesis was increased. The F4/80 immunohistochemistry effectively stained macrophage cytoplasm and allowed us to observe TAMs in the tumor. F4/80+ TAMs were commonly observed in the perivascular region of blood vessel channels within tumors. The TAM densities were 12.1% and 27.6% in the control and rhTSH groups, respectively, and significantly increased in rhTSH group ($P = 0.004$; Figure 16).

(A)

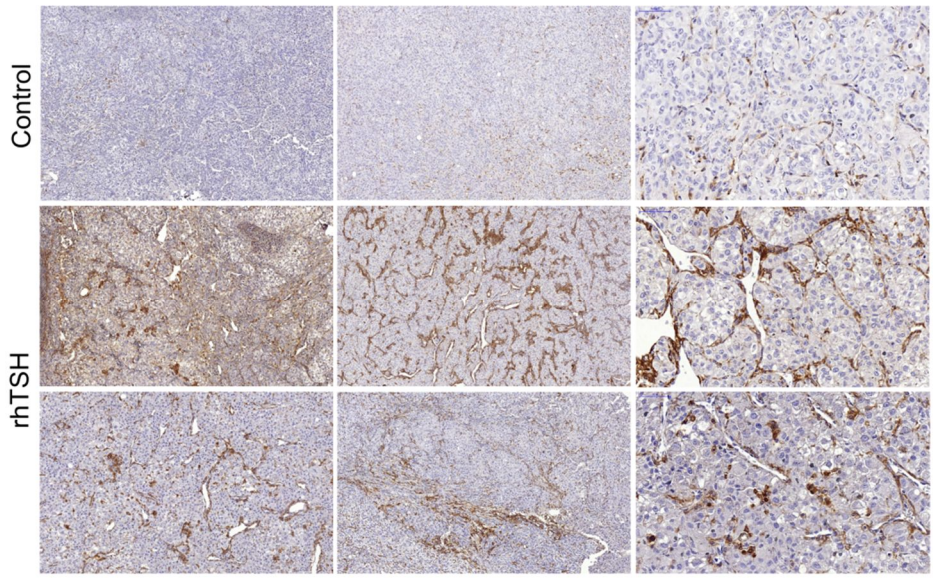

(B)

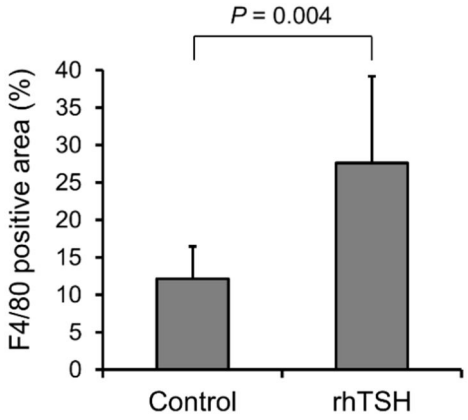

Figure 16. Effects of TSH on the recruitments of tumor-associate macrophages (TAMs).

(A) Immunohistochemical staining of F4/80. TAMs were identified as F4/80 positive cells (brownish) with thin and elongated cytoplasmic extensions that formed a canopy structure over tumor cells (left and middle, ×200; right, ×400). (B) Comparison of F4/80 positive area (%) in thyroid cancer tissues of the control and rhTSH groups. TAMs were scored by the number of F4/80+ cells/total tumor cells under ×400 magnification.

5. In vitro effects of TSH on angiogenesis

BHP10-3SC and FRO cells were cultured in the absence and presence of TSH for 24, 48, and 72 hours and evaluated for the VEGF-A mRNA expression. In BHP10-3SC cells, VEGF-A expression was up-regulated as TSH concentration and time increased (*P* for control vs. TSH 20 ng/μl treatment at 48 h = 0.030; *P* for control vs. TSH 2 ng/μl treatment at 72 h = 0.016; *P* for control vs. TSH 20 ng/μl treatment at 72 h = 0.001). Interestingly, TSH did not stimulate VEGF-A expression in TSH-independent FRO cells (Figure 17). This result suggests that TSH is a regulator of VEGF expression in DTC cells, while other growth factors, such as epidermal growth factors, may play a role in regulating VEGF expression and angiogenesis in undifferentiated thyroid cancer cells as previously reported (41).

Next, protein levels of VEGF-A were measured by ELISA method. BHP10-3SC cells were treated with TSH (20 ng/μl) or saline for 24 or 72 h and conditioned medium (CM) was harvested. VEGF-A level was higher in TSH-CM than control-CM at 24 h (12.8 ± 1.3 vs. 4.9 ± 1.1 ng/ml, *P* = 0.025), and this difference was weakened at 72 h (18.9 ± 0.9 vs. 16.0 ± 0.7 ng/ml, *P* = 0.079). Therefore, the CM at 24 h was used for cell migration and tube

formation assays.

To explore the effects of TSH on endothelial cells, cell migration and tube formation potentials were analyzed using HMVEC and HUVEC. In TSH-CM group, the endothelial cell migration was enhanced compared to control-CM (25.3 ± 1.5% vs. 5.2 ± 0.3%, $P = 0.005$ in HMVEC; 37.8 ±1.0% vs. 11.9 ± 0.7%, $P = 0.001$ in HUVEC; Figures 18A and B) as happened with tube formation (16.7 ± 0.9 vs. 4.0 ± 0.6, $P < 0.001$ in HMVEC; 24.0 ±1.7 vs. 6.7 ± 0.3, $P = 0.001$ in HUVEC; Figures 18C and D).

(A)

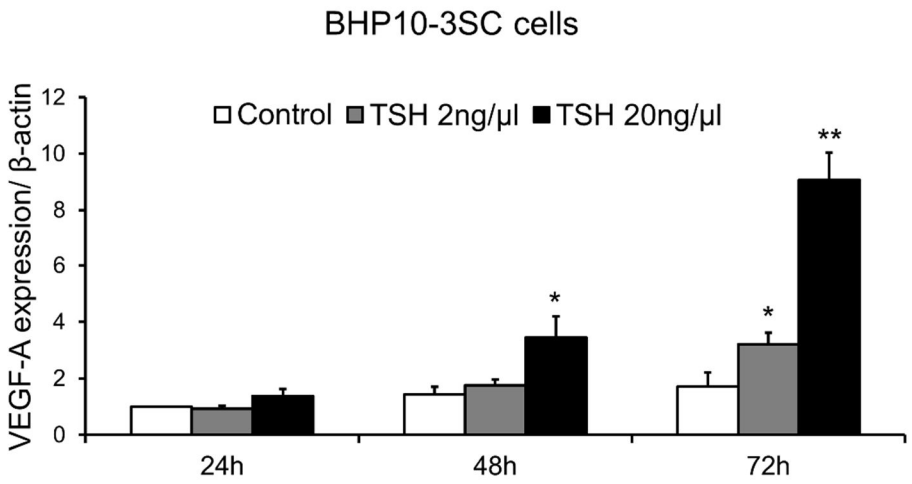

(B)

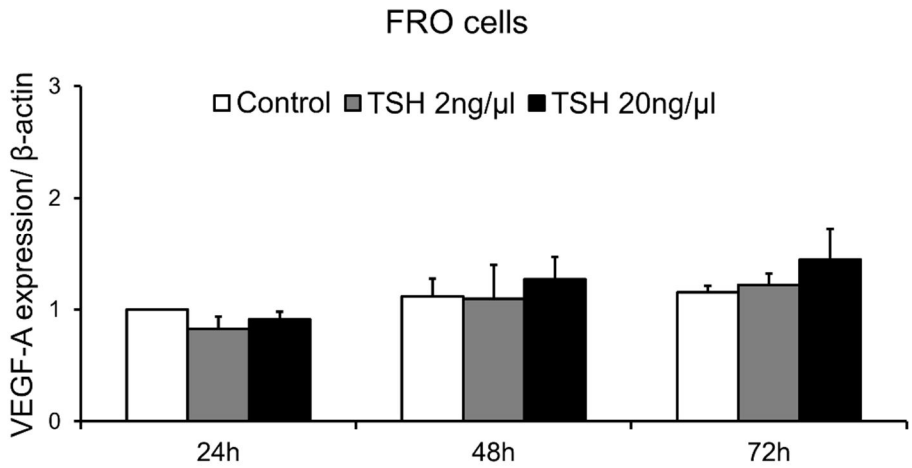

Figure 17. In vitro effects of TSH on VEGF expression in well-differentiated and poorly-differentiated thyroid cancer cells.

BHP10-3SC (A) and FRO (B) cells were culture in the absence and presence of TSH (0, 2, 20 ng/ul) for 24-72 hours and evaluated for mRNA expression of VEGF-A. *P*-values indicate the statistical significance of VEGF-A expression comparing with the untreated control at the same time. Data are shown as mean ± standard deviation of triplicates from two independent experiments. **P* <0.05, ***P* <0.01.

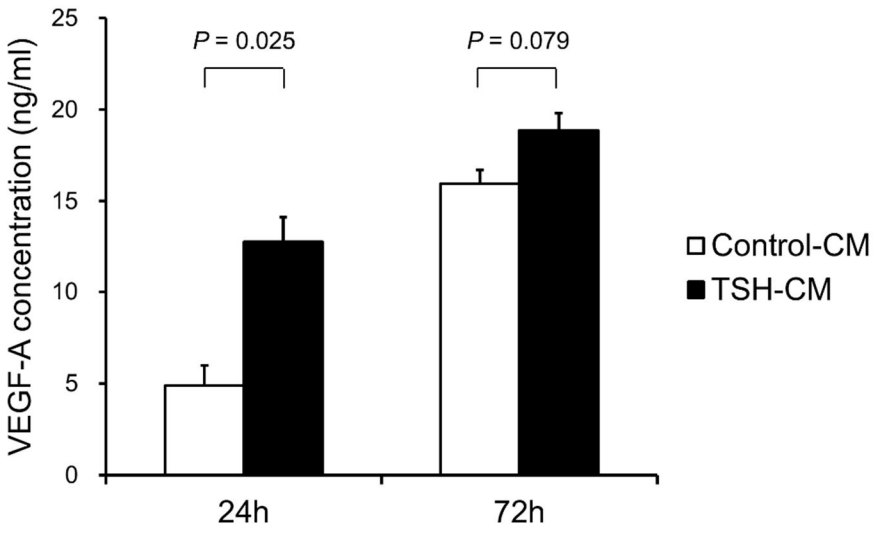

Figure 18. In vitro effects of TSH on the protein levels of VEGF-A

BHP10-3SC cells were treated with TSH (20 ng/μl) or saline for 24 or 72 h and conditioned medium (CM) was harvested. Comparisons of VEGF-A concentration (ng/ml) between saline-treated CM (control-CM) and TSH-treated CM (TSH-CM). Data are presented as mean ± standard deviation from duplicate results.

(A)

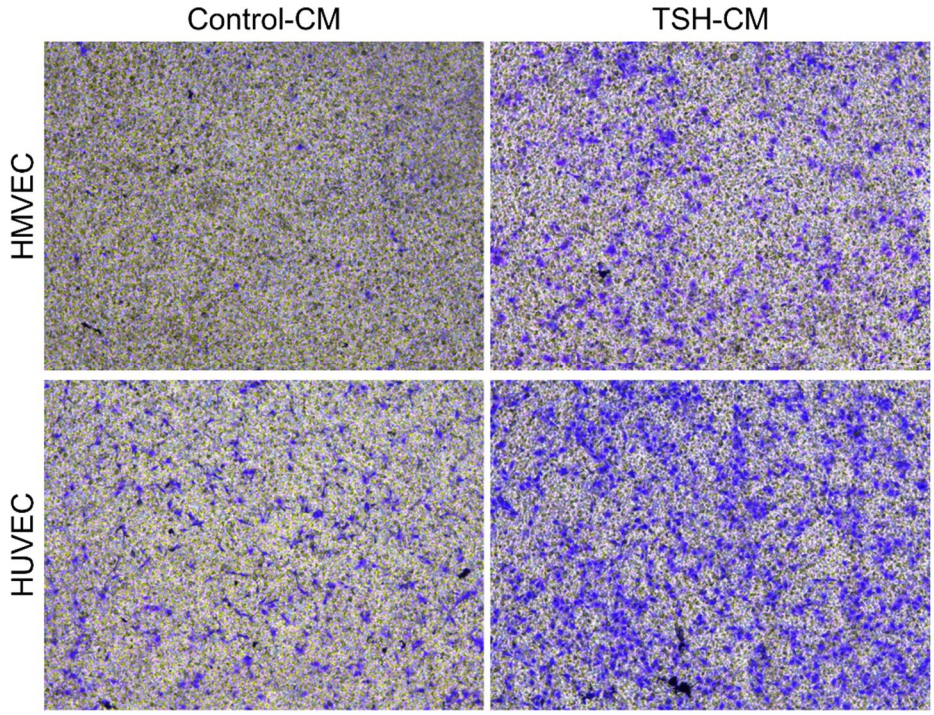
Control-CM
TSH-CM
HMVEC
HUVEC

(B)

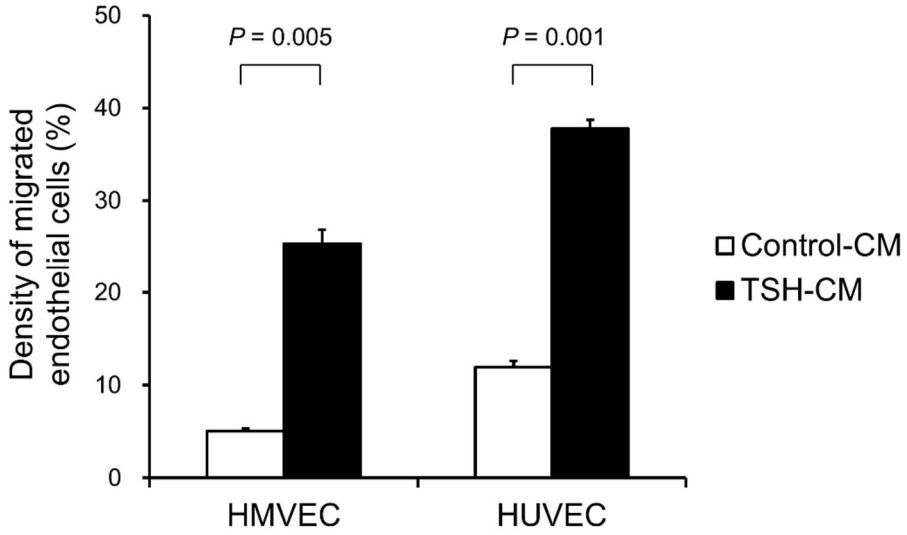
P = 0.005
P = 0.001
Density of migrated endothelial cells (%)
50
40
30
20
10
0
HMVEC
HUVEC
Control-CM
TSH-CM

(C)

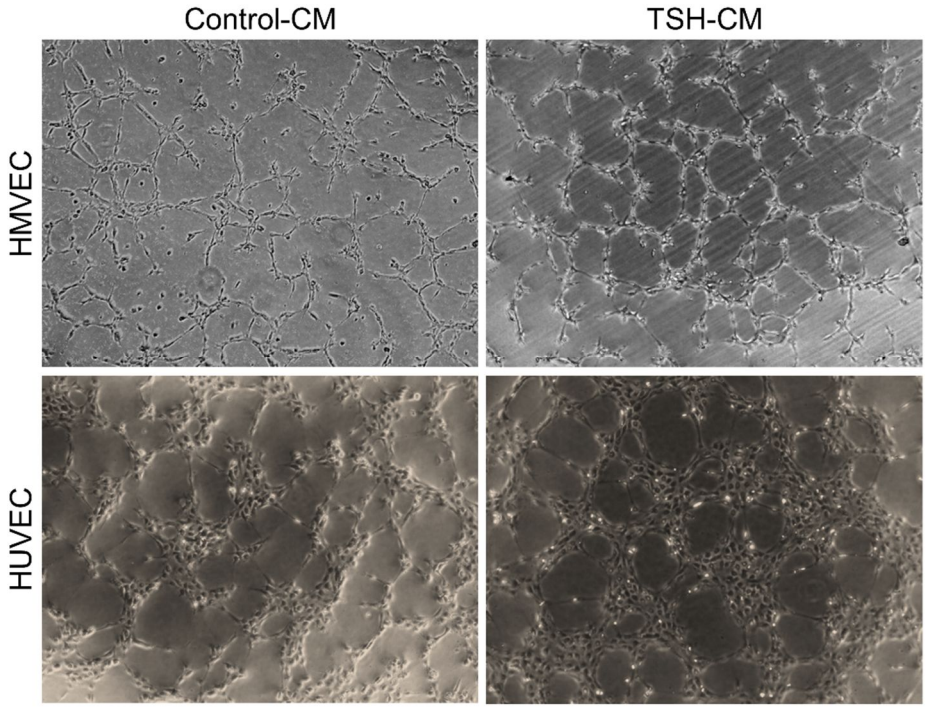

(D)

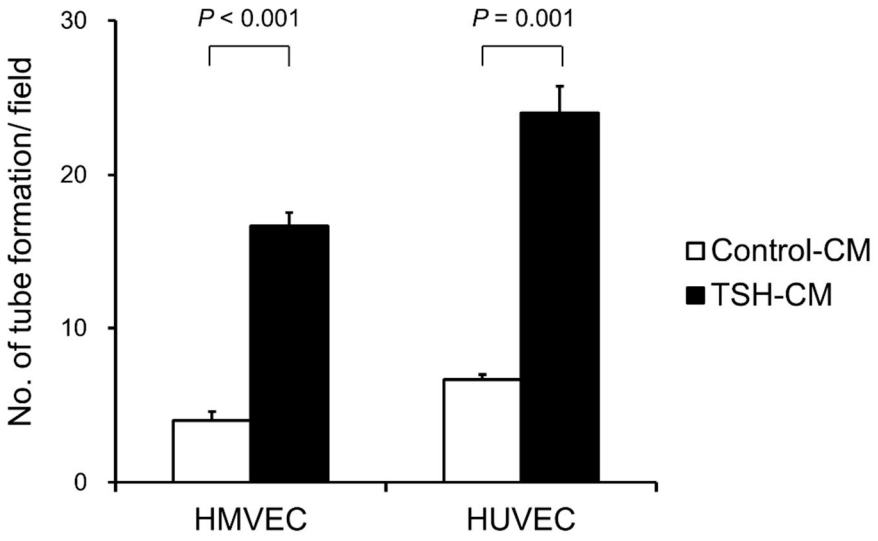

Figure 19. In vitro effects of TSH on angiogenesis

(A) Conditioned medium of saline-treated BHP10-3SC cells (control-CM) or TSH-treated CM (TSH-CM) was harvested at 24 h. HMVEC and HUVEC cells, which represent human microvascular and macrovascular endothelial cells, respectively, were treated with control-CM and TSH-CM, and transwell migration assay was performed. Migrating cells were stained with 1% crystal violet solutions and observed at 4 h. (B) Comparisons of the migrated cell density (%) in three randomly selected fields (×100) between control-CM and TSH-CM. (C) HMVEC and HUVEC cells were cultured in Matrigel-coated plate with control-CM and TSH-CM. The tube lengths were observed at 3 h. (D) Comparisons of the number of tube formation measured in three randomly selected fields (×100) between control-CM and TSH-CM.

DISCUSSION

In this study, we demonstrated that TSH enhanced tumor angiogenesis as well as TAM recruitment in thyroid cancer tissues, and identified the effects of TSH on thyroid cancer progression by modulating tumor microenvironment by *in vivo* studies.

Administration of rhTSH stimulated both macroscopic and microscopic vasculature development in thyroid cancer. This upregulated tumor angiogenesis was characterized by tortuous and dilated vasculatures. In normal tissue, the blood vessels have normal structure and function because of balance of the signals downstream of the proangiogenic molecules (e.g., VEGF and angiopoietin-2) and antiangiogenic molecules (e.g., sVEGFR1, thrombospondins, and semaphorins). In contrast, tumor vessels are structurally and functionally abnormal because of an imbalance between pro- and antiangiogenic signals. This creates an abnormal microenvironment in tumors, characterized by hypoxia, acidosis, and elevated fluid pressure, that fuels tumor progression and treatment resistance through multiple mechanisms. Therefore, as alleviating abnormal tumor microenvironment has been highlighted, the recent anti-angiogenic therapies have been focusing on vascular normalization rather than simply reducing blood vessel

number and blood flow (42).

Our results showed that CD4/80-positive macrophage density was significantly increased with tumor progression by rhTSH administration. This finding suggests a potential pro-tumorigenic role of TAMs in thyroid cancer. TAMs have been found to play dual actions, both pro- and anti-tumorigenic functions, depending on tumor microenvironments (17, 43, 44). Meanwhile, recent experimental studies in thyroid cancer were more focused on pro-tumorigenic roles of TAMs (33-35). TAMs are one of the major components of tumor microenvironment and play pivotal roles in tumor growth, metastasis and angiogenesis. The hypoxic tumor microenvironment induces recruitment of TAMs and polarizes them to the immune inhibitory M2-like phenotype (45). Furthermore, these immunosuppressive TAMs contribute to maintain the abnormal tumor vasculature (30). Thus, therapeutic targeting of modulating tumor microenvironment including angiogenesis and TAMs in human thyroid cancer may represent a valuable strategy.

VEGF, a vascular endothelial cell specific mitogen, has been identified as a major mediator of angiogenesis in the thyroid gland. Recently, tyrosin kinase inhibitor (TKI)-induced hypothyroidism has become a problem. The

proposed mechanism explaining association of thyroid dysfunction is that the TKIs, such as sunitinb and bevacizumab, target VEGF/VEGF-R pathway and may reduce the thyroid microvasculatures leading to tissue ischemia and decreasing blood flow to the thyroid gland. Therefore, we postulated VEGF might play a major role in thyroid cancer angiogenesis like in thyroid gland. Our results showed a significant upregulation of VEGF secretion by TSH *in vitro*, but did not show significant differences *in vivo*. Additional confirmation of VEGF expression by using protein detection methods such as Western blots, ELISA, and IHC, rather than RNA real-time PCR is required. Moreover, this result suggests that the growth factors and cytokines other than VEGF might be involved in TSH-induced angiogenesis. Thus, further studies are needed to assess other proangiogenic factors mediating the action of TSH.

Tumor angiogenesis features leaky and immature blood vessels (46, 47). Leaky blood vessels limit vascular perfusion resulting in a hypoxic microenvironment and a resistance to cytotoxic chemotherapy. We observed the increased hemorrhage in gross findings of tumors in rhTSH group, and the dilated and tortuous vasculatures in microscopic findings of them. However, we failed to find a significant increase in endothelial fenestration

by electron microscopy and could not distinguish it from an increment in vascular density by distribution of FITC-labeled nanoparticles. Tumors commonly exhibit heterogeneous perivascular cells with abnormal morphology (47). Therefore, further investigation for functionally demonstrating the TSH effects on tumor vascular permeability is required.

The limitation of this study is that serum thyroid hormone levels were elevated in rhTSH group. Excluding thyroid hormone effects would be important for accurate assessment of the effects of TSH alone. Thus, we are planning to add the propylthiouracil (PTU) and T3-treated groups for the exclusion of confounding effects of thyroid hormone. We can expect that the mice treated with PTU, a drug used to treat hyperthyroidism by decreasing thyroid hormone production, have lower serum thyroid hormone level and elevated TSH level by negative feedback. Treatment of T3 induces contrary status with PTU; serum thyroid hormone level are increased while TSH level decreased.

In conclusion, TSH stimulated tumor growth via enhancing abnormal vascular formation and subsequent recruitment of macrophages in thyroid cancer. Modulating tumor microenvironment may be one of the mechanisms of TSH-induced tumor growth in DTC.

REFERENCES

1. Boelaert K, Horacek J, Holder RL, Watkinson JC, Sheppard MC, Franklyn JA. Serum thyrotropin concentration as a novel predictor of malignancy in thyroid nodules investigated by fine-needle aspiration. J Clin Endocrinol Metab. 2006;91(11):4295-301.
2. Jonklaas J, Nsouli-Maktabi H, Soldin SJ. Endogenous thyrotropin and triiodothyronine concentrations in individuals with thyroid cancer. Thyroid. 2008;18(9):943-52.
3. Polyzos SA, Kita M, Efstathiadou Z, Poulakos P, Slavakis A, Sofianou D, et al. Serum thyrotropin concentration as a biochemical predictor of thyroid malignancy in patients presenting with thyroid nodules. J Cancer Res Clin Oncol. 2008;134(9):953-60.
4. Fiore E, Rago T, Provenzale MA, Scutari M, Ugolini C, Basolo F, et al. Lower levels of TSH are associated with a lower risk of papillary thyroid cancer in patients with thyroid nodular disease: thyroid autonomy may play a protective role. Endocr Relat Cancer. 2009;16(4):1251-60.
5. Haymart MR, Glinberg SL, Liu J, Sippel RS, Jaume JC, Chen H. Higher serum TSH in thyroid cancer patients occurs independent of age and correlates with extrathyroidal extension. Clin Endocrinol (Oxf). 2009;71(3):434-9.
6. Haymart MR, Repplinger DJ, Leverson GE, Elson DF, Sippel RS, Jaume JC, et al. Higher serum thyroid stimulating hormone level in thyroid nodule patients is associated with greater risks of differentiated thyroid cancer and advanced tumor stage. J Clin Endocrinol Metab. 2008;93(3):809-14.
7. Hovens GC, Stokkel MP, Kievit J, Corssmit EP, Pereira AM, Romijn JA,

et al. Associations of serum thyrotropin concentrations with recurrence and death in differentiated thyroid cancer. J Clin Endocrinol Metab. 2007;92(7):2610-5.

8. Jonklaas J, Sarlis NJ, Litofsky D, Ain KB, Bigos ST, Brierley JD, et al. Outcomes of patients with differentiated thyroid carcinoma following initial therapy. Thyroid. 2006;16(12):1229-42.
9. American Thyroid Association Guidelines Taskforce on Thyroid N, Differentiated Thyroid C, Cooper DS, Doherty GM, Haugen BR, Kloos RT, et al. Revised American Thyroid Association management guidelines for patients with thyroid nodules and differentiated thyroid cancer. Thyroid. 2009;19(11):1167-214.
10. Pacini F, Schlumberger M, Dralle H, Elisei R, Smit JW, Wiersinga W, et al. European consensus for the management of patients with differentiated thyroid carcinoma of the follicular epithelium. Eur J Endocrinol. 2006;154(6):787-803.
11. Sundram F, Robinson BG, Kung A, Lim-Abrahan MA, Bay NQ, Chuan LK, et al. Well-differentiated epithelial thyroid cancer management in the Asia Pacific region: a report and clinical practice guideline. Thyroid. 2006;16(5):461-9.
12. Duh QY, Siperstein AE, Miller RA, Smeds S, Clark OH. TSH binding correlates with TSH-stimulated thyroid adenylate cyclase activity in human thyroid tissues. Surgery. 1989;106(6):967-73; discussion 73-4.
13. Shaver JK, Tezelman S, Siperstein AE, Duh QY, Clark OH. Thyroid-stimulating hormone activates phospholipase C in normal and neoplastic thyroid tissue. Surgery. 1993;114(6):1064-9.
14. Duh QY, Grossman RF. Thyroid growth factors, signal transduction pathways, and oncogenes. Surg Clin North Am. 1995;75(3):421-37.
15. Hoelting T, Tezelman S, Siperstein AE, Duh QY, Clark OH. Thyrotropin stimulates invasion and growth of follicular thyroid cancer cells via

PKC- rather than PKA-activation. Biochem Biophys Res Commun. 1993;195(3):1230-6.

16. Zielke A, Hoffmann S, Plaul U, Duh QY, Clark OH, Rothmund M. Pleiotropic effects of thyroid stimulating hormone in a differentiated thyroid cancer cell line. Studies on proliferation, thyroglobulin secretion, adhesion, migration and invasion. Exp Clin Endocrinol Diabetes. 1999;107(6):361-9.
17. Coussens LM, Werb Z. Inflammation and cancer. Nature. 2002;420(6917):860-7.
18. Leung DW, Cachianes G, Kuang WJ, Goeddel DV, Ferrara N. Vascular endothelial growth factor is a secreted angiogenic mitogen. Science. 1989;246(4935):1306-9.
19. Carmeliet P. VEGF as a key mediator of angiogenesis in cancer. Oncology. 2005;69 Suppl 3:4-10.
20. Hoeben A, Landuyt B, Highley MS, Wildiers H, Van Oosterom AT, De Bruijn EA. Vascular endothelial growth factor and angiogenesis. Pharmacol Rev. 2004;56(4):549-80.
21. Fenton C, Patel A, Dinauer C, Robie DK, Tuttle RM, Francis GL. The expression of vascular endothelial growth factor and the type 1 vascular endothelial growth factor receptor correlate with the size of papillary thyroid carcinoma in children and young adults. Thyroid. 2000;10(4):349-57.
22. Klein M, Vignaud JM, Hennequin V, Toussaint B, Bresler L, Plenat F, et al. Increased expression of the vascular endothelial growth factor is a pejorative prognosis marker in papillary thyroid carcinoma. J Clin Endocrinol Metab. 2001;86(2):656-8.
23. Lennard CM, Patel A, Wilson J, Reinhardt B, Tuman C, Fenton C, et al. Intensity of vascular endothelial growth factor expression is associated with increased risk of recurrence and decreased disease-free survival in

papillary thyroid cancer. Surgery. 2001;129(5):552-8.

24. Hoffmann S, Hofbauer LC, Scharrenbach V, Wunderlich A, Hassan I, Lingelbach S, et al. Thyrotropin (TSH)-induced production of vascular endothelial growth factor in thyroid cancer cells in vitro: evaluation of TSH signal transduction and of angiogenesis-stimulating growth factors. J Clin Endocrinol Metab. 2004;89(12):6139-45.
25. Soh EY, Sobhi SA, Wong MG, Meng YG, Siperstein AE, Clark OH, et al. Thyroid-stimulating hormone promotes the secretion of vascular endothelial growth factor in thyroid cancer cell lines. Surgery. 1996;120(6):944-7.
26. Sato K, Yamazaki K, Shizume K, Kanaji Y, Obara T, Ohsumi K, et al. Stimulation by thyroid-stimulating hormone and Grave's immunoglobulin G of vascular endothelial growth factor mRNA expression in human thyroid follicles in vitro and flt mRNA expression in the rat thyroid in vivo. J Clin Invest. 1995;96(3):1295-302.
27. Klein M, Brunaud L, Muresan M, Barbe F, Marie B, Sapin R, et al. Recombinant human thyrotropin stimulates thyroid angiogenesis in vivo. Thyroid. 2006;16(6):531-6.
28. Li J, Teng L, Jiang H. Relationship between preoperative serum TSH levels and expression of VEGF in papillary thyroid carcinoma. Asia Pac J Clin Oncol. 2014;10(2):149-52.
29. Gajewski TF, Schreiber H, Fu YX. Innate and adaptive immune cells in the tumor microenvironment. Nat Immunol. 2013;14(10):1014-22.
30. Solinas G, Germano G, Mantovani A, Allavena P. Tumor-associated macrophages (TAM) as major players of the cancer-related inflammation. J Leukoc Biol. 2009;86(5):1065-73.
31. Bingle L, Brown NJ, Lewis CE. The role of tumour-associated macrophages in tumour progression: implications for new anticancer therapies. J Pathol. 2002;196(3):254-65.

32. Zeni E, Mazzetti L, Miotto D, Lo Cascio N, Maestrelli P, Querzoli P, et al. Macrophage expression of interleukin-10 is a prognostic factor in nonsmall cell lung cancer. Eur Respir J. 2007;30(4):627-32.
33. Kim S, Cho SW, Min HS, Kim KM, Yeom GJ, Kim EY, et al. The expression of tumor-associated macrophages in papillary thyroid carcinoma. Endocrinol Metab (Seoul). 2013;28(3):192-8.
34. Ryder M, Ghossein RA, Ricarte-Filho JC, Knauf JA, Fagin JA. Increased density of tumor-associated macrophages is associated with decreased survival in advanced thyroid cancer. Endocr Relat Cancer. 2008;15(4):1069-74.
35. Qing W, Fang WY, Ye L, Shen LY, Zhang XF, Fei XC, et al. Density of tumor-associated macrophages correlates with lymph node metastasis in papillary thyroid carcinoma. Thyroid. 2012;22(9):905-10.
36. Ahn SH, Henderson Y, Kang Y, Chattopadhyay C, Holton P, Wang M, et al. An orthotopic model of papillary thyroid carcinoma in athymic nude mice. Arch Otolaryngol Head Neck Surg. 2008;134(2):190-7.
37. Mo JH, Choi IJ, Jeong WJ, Jeon EH, Ahn SH. HIF-1alpha and HSP90: target molecules selected from a tumorigenic papillary thyroid carcinoma cell line. Cancer Sci. 2012;103(3):464-71.
38. Kim KS, Min JK, Liang ZL, Lee K, Lee JU, Bae KH, et al. Aberrant l1 cell adhesion molecule affects tumor behavior and chemosensitivity in anaplastic thyroid carcinoma. Clin Cancer Res. 2012;18(11):3071-8.
39. Colzani RM, Alex S, Fang SL, Braverman LE, Emerson CH. The effect of recombinant human thyrotropin (rhTSH) on thyroid function in mice and rats. Thyroid. 1998;8(9):797-801.
40. Tomayko MM, Reynolds CP. Determination of subcutaneous tumor size in athymic (nude) mice. Cancer Chemother Pharmacol. 1989;24(3):148-54.
41. Landriscina M, Piscazzi A, Fabiano A, Maddalena F, Costantino E,

Farese A, et al. Targeting epidermal growth factor receptor 1 signaling in human thyroid-stimulating hormone-independent thyroid carcinoma FRO cells results in a more chemosensitive and less angiogenic phenotype. Thyroid. 2009;19(6):629-37.

42. Jain RK. Antiangiogenesis strategies revisited: from starving tumors to alleviating hypoxia. Cancer Cell. 2014;26(5):605-22.
43. Zhang QW, Liu L, Gong CY, Shi HS, Zeng YH, Wang XZ, et al. Prognostic significance of tumor-associated macrophages in solid tumor: a meta-analysis of the literature. PLoS One. 2012;7(12):e50946.
44. Pollard JW. Tumour-educated macrophages promote tumour progression and metastasis. Nat Rev Cancer. 2004;4(1):71-8.
45. Heusinkveld M, van der Burg SH. Identification and manipulation of tumor associated macrophages in human cancers. J Transl Med. 2011;9:216.
46. Jain RK. Normalization of tumor vasculature: an emerging concept in antiangiogenic therapy. Science. 2005;307(5706):58-62.
47. Fukumura D, Jain RK. Tumor microvasculature and microenvironment: targets for anti-angiogenesis and normalization. Microvasc Res. 2007;74(2-3):72-84.

국문초록

갑상선자극호르몬이 종양 미세환경 조절을 통해 갑상선암의 성장에 미치는 영향

서울대학교 대학원 의학과 중개의학 전공

송 영 신

서론: 갑상선자극호르몬은 수용체를 통하여 갑상선 세포의 성장을 촉진하는 것으로 알려져 있다. 분화 갑상선암에는 갑상선자극호르몬 수용체가 존재하며, 갑상선자극호르몬에 의해 암세포 성장이 촉진될 수 있다. 이러한 근거를 바탕으로 '갑상선자극호르몬 억제 요법'이 분화 갑상선암 환자들에게 중요한 치료 전략으로 사용되어왔다. 혈관신생을 포함한 종양 미세환경의 변화는 암세포의 성장 및 전이 과정에 필수적인 역할을 한다. 따라서, 본 연구에서는 분화 갑상선암 마우스 모델을 이용하여 갑상선자극호르몬이 종양 미세환경 조절을 통해

갑상선암의 성장에 미치는 영향에 대해 알아보고자 하였다.

방법: 7주령의 BALB/c nu/nu 마우스에 분화 갑상선암 세포주인 BHP10-3SC 세포를 피하 이식하였다. 종양이 육안적으로 보이기 시작하는 시점부터 치료군에는 갑상선자극호르몬을, 대조군에는 생리식염수를 매일 복강 내 투여하였다. 종양의 크기는 3일 간격으로 측정하였다. 15일간 투약한 후에 종양의 조직학적 소견 및 혈관내피성장인자(VEGF) mRNA 발현을 확인하였다. In vivo 실험 결과를 보충하기 위해 BHP10-3SC 세포와 혈관 내피 세포를 이용한 in vitro 실험을 추가로 시행하였다.

결과: 갑상선자극호르몬은 종양의 크기 성장을 유의하게 촉진하였다 (1733.4 ± 793.5 mm^3 vs. 1148.8 ± 471.1 mm^3, P = 0.010). 갑상선자극호르몬을 투여한 군이 대조군에 비해 종양 혈관의 밀도가 더 높을 뿐만 아니라 (13.8 ± 0.8% vs. 5.7 ± 0.8%, P = 0.021), 더욱 굴곡이 있고 팽창되어있는 모습이 관찰되었다 (혈관 직경 23.0 ± 1.7 μm vs. 7.4 ± 0.5 μm, P <0.001). 또한, 종양 대식세포 침윤이 유의하게 증가된 소견이 관찰되었다 (27.6 ± 11.6% vs. 12.1 ± 4.3%, P = 0.004). In vitro 실험에서는 갑상선자극호르몬을 BHP10-SC 세포에 처리하였을 때 VEGF-A mRNA 발현이 대조군에 비해 유의하게 증가하는 소견을 보였다.

갑상선자극호르몬을 처리한 배지에서 VEGF-A 단백의 농도가 더 높았고, 이 배지를 혈관 내피 세포에 처리하였을 때 세포 이동 및 혈관 형성이 증가함을 확인하였다.

결론: 갑상선자극호르몬은 갑상선암의 비정상적인 혈관 형성 및 이에 따른 대식세포의 침윤을 증가시켜 종양 성장을 촉진하였다. 갑상선자극호르몬이 종양 미세환경을 조절하여 분화 갑상선암의 성장을 유도하는 새로운 작용 기전을 규명하였다.

주요어: 갑상선자극호르몬, 갑상선암, 암의 성장, 혈관신생, 미세환경, 대식세포

학번: 2014-21161